

Combustion Characteristics of an Ammonium-Dinitramide-Based Ionic Liquid Propellant

By Yuichiro IDE,¹⁾ Takuya TAKAHASHI,²⁾ Keiichiro IWAI,²⁾ Katsuhiko NOZOE,²⁾ Hiroto HABU³⁾ and Shinichiro TOKUDOME^{1), 3)}

¹⁾ Department of Space and Astronautical Science, SOKENDAI (The Graduate University for Advanced Studies), Sagami-hara, Japan

²⁾ Carlit Holdings Co., Ltd., Tokyo, Japan

³⁾ Institute of Space and Astronautical Science, JAXA, Sagami-hara, Japan

(Received July 31st, 2015)

As a replacement for hydrazine, ammonium-dinitramide-based ionic liquid propellant (ADN-based ILP) has been developed by JAXA and Carlit Holdings Co., Ltd. This propellant is made by mixing three solid powders: ADN, monomethylamine nitrate, and urea. The propellant's theoretical specific impulse is 1.2 times higher than that of hydrazine, and its density is 1.5 times higher at a certain composition. Although ionic liquids were believed to be non-flammable for a long time owing to their low-volatility, recently combustible ILs have been reported. The combustion mechanism of ILs is not yet understood. The objective of this paper is to understand the combustion wave structure of ADN-based ILP. The temperature distribution of the combustion wave in a strand burner test shows a region of constant temperature. This region would indicate boiling in a gas-liquid phase. Thus, the combustion wave structure consists of liquid, gas-liquid, and gas phases. The dependence of boiling point on pressure would identify chemical substances in the gas-liquid phase. The dependence of combustion and ignition characteristics on ADN content is also discussed.

Key Words: Ammonium dinitramide, Combustion wave structure, Ionic liquids, Monopropellants, Strand burner tests

Nomenclature

a	: proportionality constant relevant to dependence of linear burning rate on pressure
c_p	: specific heat at constant pressure
G	: gas phase
L	: liquid phase
n	: pressure exponent
P	: pressure in strand burner
r	: linear burning rate
T_f	: flame temperature
T_{ad}	: adiabatic flame temperature
v_G	: burning rate of gas
λ	: heat conductivity
ω	: chemical reaction rate
ρ	: density

Subscripts

G	: gas phase
L	: liquid phase

1. Introduction

Low-toxicity and high-performance liquid propellants are required as alternatives to hydrazine. Because of hydrazine's toxicity, it is expensive to manufacture and operate spacecraft in terms of their propulsion systems.¹⁾ In order to improve this problem, hydroxylammonium-nitrate-based (HAN-based) solutions and ammonium-dinitramide-based (ADN-based) solutions have been studied as prospective candidates.^{2,3)}

JAXA and Carlit Holdings Co., Ltd. have developed an ADN-based ionic liquid propellant (ADN-based ILP) as one of the prospective candidates. This compound consists of ADN, monomethylamine nitrate (MMAN), and urea. After mixing the three solid powders, the mixture becomes liquid owing to freezing-point depression. Therefore, it contains no water. The propellant's theoretical specific impulse is 1.2 times higher than that of hydrazine and its density is 1.5 times higher at a certain composition.

According to our past studies, the prospective composition was selected at 10 wt. % intervals as ADN/MMAN/Urea=30/50/20 wt. %, and self-sustaining combustion was confirmed in an inert atmosphere.⁴⁾ The linear burning rate and flame temperature were measured as basic combustion characteristics.

The ADN-based ILP is similar to other ionic liquids (ILs), which are salts with melting points below 373 K;⁵⁾ it has low-volatility and contains ions of ADN and MMAN. Because of their low-volatility, ILs were believed to be non-flammable for a long time. However, some papers reported that certain ILs can burn.⁶⁾ Although thermal decomposition and measurement of flash point were researched with respect to ILs,^{7,8)} the combustion mechanism of ILs has not yet been determined.

The objective of this paper is to understand the combustion wave structure in order to research the combustion mechanism of the ADN-based ILP. Combustion and ignition characteristics are also discussed. In particular, the dependence on ADN content are focused on because ADN is a well-known highly energetic oxidizer.

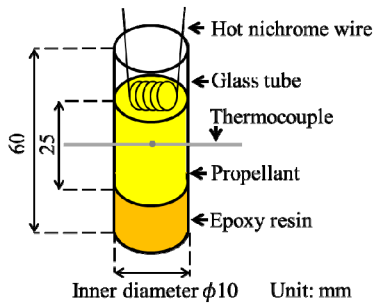


Fig. 1. Schematic representation of a setup in strand burner test. The propellant was heated until its ignition. Joule heat from the coiled part of the wire was about 12 W. Heating time ranged from 0.5 to 28 s, depending on ambient pressure and propellant composition.

In this work, strand burner tests were conducted for investigating quasi-one-dimensional combustion wave structure. The strand burner test is a basic classical method for measuring the burning rate of hydrazine and HAN-based monopropellants^{9,10} and is sometimes used for measurement of temperature profiles.¹¹ The combustion wave structure of the ADN-based ILP is discussed in terms of the temperature profile of the combustion wave, images of combustion, and other results.

2. Experimental Conditions

The strand burner tests of the ADN-based ILP were conducted at pressures in the range of 0.15 to 3.0 MPa. The ADN-based ILP was poured into a glass tube and ignited directly by hot nichrome wire. The linear burning rate (i.e., regression rate of the liquid surface) was measured by motion pictures of the combustion. Temperature in the combustion wave was measured by a Pt/Pt-13%Rh-type thermocouple with a 25- μ m diameter, which was set up to penetrate the glass tube as shown in Fig. 1. Compositions of the ADN-based ILP were selected to research the effect of ADN content as ADN/MMAN/Urea=30/50/20, 35/45/20, and 40/40/20 wt. % on the basis of the prospective composition of 30/50/20 wt. %. The other reason for these selections is to research the effect of the highly energetic materials ADN and MMAN with a constant content of urea.

3. Results

Combustion and ignition characteristics are the results of the strand burner tests.

3.1. Combustion characteristics

The linear burning rates and flame temperatures of the ADN-based ILP are basic combustion characteristics.

First, the dependence of linear burning rate on pressure was obtained at each composition as shown in Fig. 2. According to the approximation curve, the dependence of linear burning rate on pressure is described by Eq. (1), where the proportionality constant a and the pressure exponent n increase with increasing ADN content.

$$r = aP^n \quad (1)$$

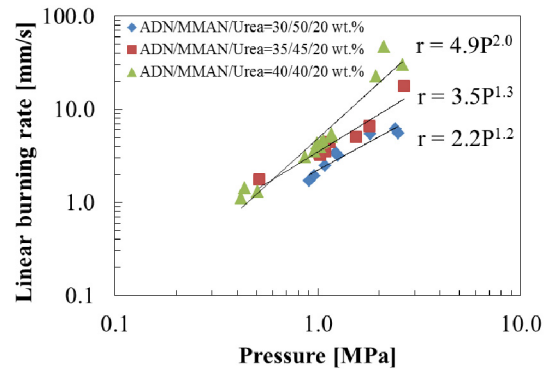


Fig. 2. Dependence of linear burning rate on pressure at each composition of ADN-based ionic liquid propellant.

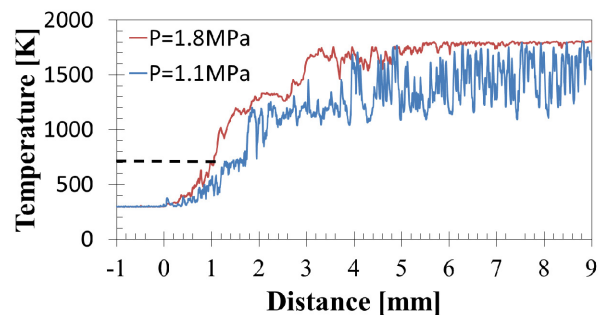


Fig. 3. Temperature distribution at a composition of ADN/MMAN/Urea=30/50/20 wt. %.

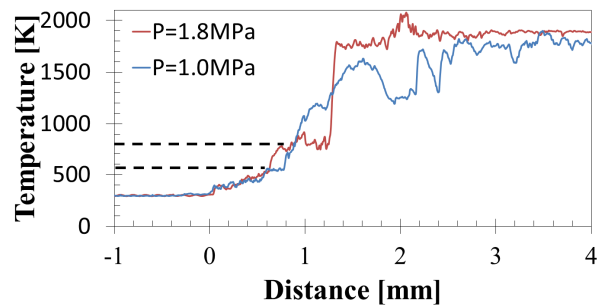


Fig. 4. Temperature distribution at a composition of ADN/MMAN/Urea=35/45/20 wt. %.

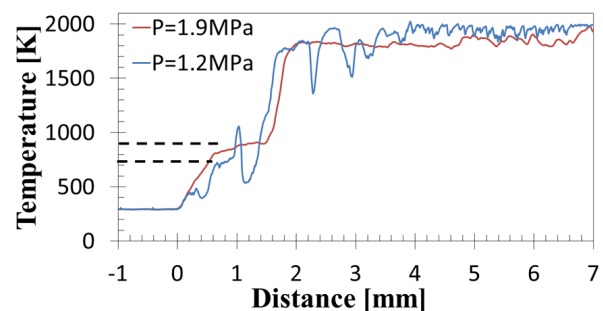


Fig. 5. Temperature distribution at a composition of ADN/MMAN/Urea=40/40/20 wt. %.

Meanwhile, temperature distributions were calculated from the measured temperature-time histories and linear burning rates as shown in Figs. 3–5. The origins of the abscissa axes in Figs. 3–5 are defined as positions where temperatures start to rise. The dashed lines denote auxiliary lines of constant

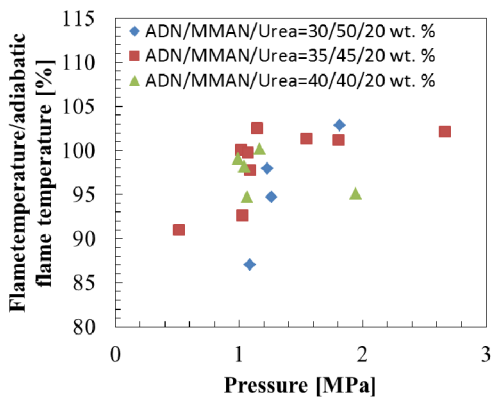


Fig. 6. Dependence of the ratio of flame temperature to adiabatic flame temperature on pressure at various compositions of ADN-based ionic liquid propellant.

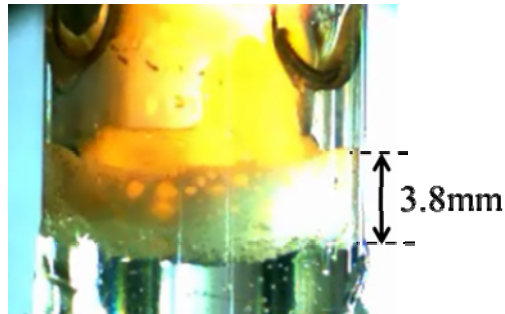


Fig. 7. Picture of a strand burner test taken with a high-speed camera at 2,000 frames per second for ADN/MMAN/Urea=40/40/20 wt. %, and $P=0.7$ MPa.

temperature in the graphs.

Figure 6 shows the dependence of T_f/T_{ad} on pressure at three compositions. T_{ad} is calculated from the heats of formation of ADN, MMAN, and urea using the NASA Chemical Equilibrium with Applications (NASA CEA) software. There is a trend where T_f/T_{ad} increases with increasing pressure. There is roughly the same trend of T_f/T_{ad} curves for all compositions. Some T_f/T_{ad} is slightly above 100% at pressures over 1 MPa. The reason for this might be lower calculated T_{ad} than true values, because the heat of melting at liquefaction of the mixture of ADN, MMAN, and urea is not considered in the calculation of T_{ad} .

Figure 7 shows a picture of a strand burner test taken by a high-speed camera at a frame rate of 2,000 frames per second. A bubble layer can be confirmed on the liquid surface.

3.2. Ignition characteristics

Behavior before ignition and the lower ignition limit, which is the lowest pressure where the propellant can burn sustainably without heat supplied by the nichrome wire, are discussed here.

The ranges of lower ignition limits are shown in Table 1. The lowest pressure in the range is the largest pressure at which self-sustaining combustion (SSC) was not confirmed, while the largest pressure in the range is the lowest pressure at

Table 1. Lower ignition limit at each composition.

ADN/MMAN/Urea [wt. %]	30/50/20	35/45/20	40/40/20
Lower ignition limit [MPa]	0.4–1.0	0.4–0.5	0.2–0.4

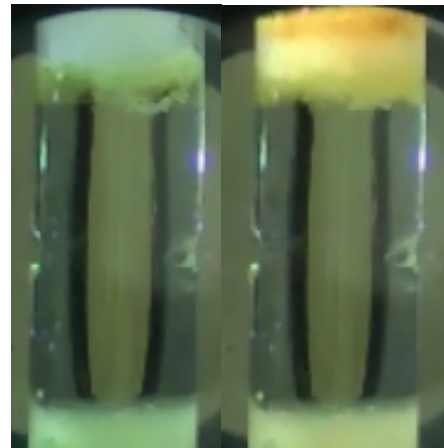


Fig. 8. Behavior of ignition at the composition of ADN/MMAN/Urea=30/50/20 wt. % and a pressure of 1.2 MPa. A white gas and a yellowish layer were formed on the liquid surface as indicated in the left image. Subsequently, three colored layers were formed on the liquid surface as indicated in the right image.

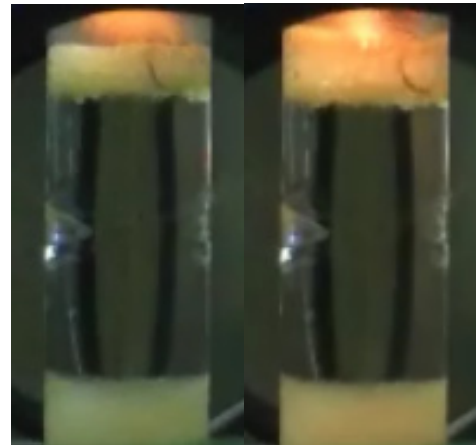


Fig. 9. Behavior of ignition at the composition of ADN/MMAN/Urea=35/45/20 wt. % and a pressure of 1.1 MPa. A white gas and a yellowish layer were formed on the liquid surface as indicated in the left image. Subsequently, three colored layers were formed on the liquid surface as indicated in the right image.

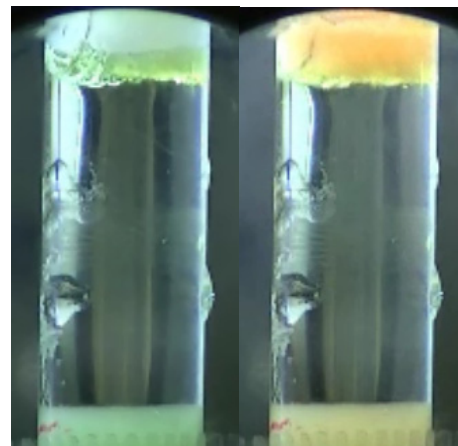


Fig. 10. Behavior of ignition at the composition of ADN/MMAN/Urea=40/40/20 wt. % and a pressure of 0.54 MPa. A white gas and a yellowish layer were formed on the liquid surface as indicated in the left image. Subsequently, two layers with pale brownish and yellowish in colors were formed on the liquid surface as indicated in the right image.

which SSC was confirmed.

Around the lower ignition limit, colored layers can be observed before ignition. A white gas was generated first from the liquid surface, and a yellowish layer was formed subsequently as indicated in the left images of Figs. 8–10. Then, the three colored layers were formed on the liquid at 30/50/20 and 35/45/20 wt. % as indicated in the right images of Figs. 8 and 9. On the other hand, two layers with pale brownish and yellowish in colors were formed on the liquid at 40/40/20 wt. % as shown in the right image of Fig. 10. After that, the layers formed a bubble layer with strong brightness at all compositions. In the case of pressures sufficiently above the lower ignition limit, only white gas was generated before ignition.

4. Discussion

This section presents a discussion of combustion wave structure, combustion characteristics with respect to the gas phase, and ignition characteristics of the ADN-based ILP in sequence on the basis of the results of the strand burner tests.

4.1. Combustion wave structure

The temperature profile of the combustion wave gives information about combustion wave structure. According to Figs. 3–5, there are regions in which temperature is constant except for the case of P=1.8 MPa in Fig. 3. These regions denote boiling of the ADN-based ILP because the temperature hardly changes although a great amount of heat must be conducted from the flame zone to the liquid phase. A foam layer over the liquid surface can be seen in all cases (e.g., Fig. 7). This is also evidence for the boiling of the ADN-based ILP. Thus, combustion wave structure consists of liquid, gas-liquid, and gas phases as shown in Fig. 11. In the liquid phase, temperature gradually increases on the flame side along the axis of the glass tube. In the gas-liquid phase, the ADN-based ILP evaporates and bubbles are generated. In the gas phase, the temperature of the evaporated gas increases rapidly and reaches the flame temperature after the reaction.

The width of the gas-liquid phase in the temperature distribution is around 0.2–1.8 mm while that of the foam layer in the photographs is around 1.0–4.5 mm. This inconsistency is due to the shape of the foam layer. According to Fig. 7, the shape of the foam would be depressed at the middle of glass tube, as a portion of foam at the back of the inner glass wall can be seen along with a flame in the middle of the depressed foam. The reason for the existence of a great amount of foam around the wall is bubble nucleation and heat loss at the wall. Thus, the width of the gas-liquid phase in the temperature distribution is narrower than that of the foam layer in the photographs because temperature was measured in the middle of the glass tube as shown in Fig. 12.

Now the behavior before ignition is discussed in terms of the mechanism of boiling. Around the lower ignition limit, a yellowish layer was observed on the ADN-based ILP before ignition (left images in Figs. 8–10). This layer might consist of decomposition products or the ADN-based ILP with less urea. In the former case, the ADN-based ILP decomposes into

volatile liquids as the yellowish layer and they vaporize into white gases. This could explain combustion of low-volatility ADN-based ILP, as one hypothesis. In the latter case, only urea contained in the ADN-based ILP is vaporized by the heat supplied from the nichrome wire because urea is a polar molecule, while ions of ADN and MMAN attract each other by strong electrostatic force. In this case, the observed white gas is urea or decomposition gases of urea.

According to this line of thought, there are some predictions as to the boiling mechanism in combustion. The first is (a) that the ADN-based ILP decomposes into volatile liquids and the vaporized products become a pre-mixed gas for combustion. The second is (b) that after urea in the ADN-based ILP vaporizes owing to its relatively weak intermolecular force, ADN and MMAN vaporize and/or are decomposed into the neutral dissociation products NH_3 , $\text{HN}(\text{NO}_2)_2$, CH_3NH_3 , and HNO_3 through endothermic reactions. The idea in (b) is based on previous research where combustion of solid ADN was successfully modeled and the combustion modeling indicated that thermal decomposition and evaporation of ADN take place in the liquid-bubble layer.¹²⁾ However, the heats of decomposition of ADN and MMAN must be endothermic in thermal decomposition because of consistency between the thermal decomposition in (b) and the existence of the regions of constant temperature. It is not clear whether or not the reactions are endothermic.

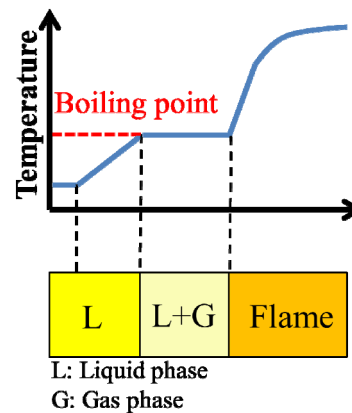


Fig. 11. Schematic representation of the combustion wave structure of the ADN-based ionic liquid propellant.

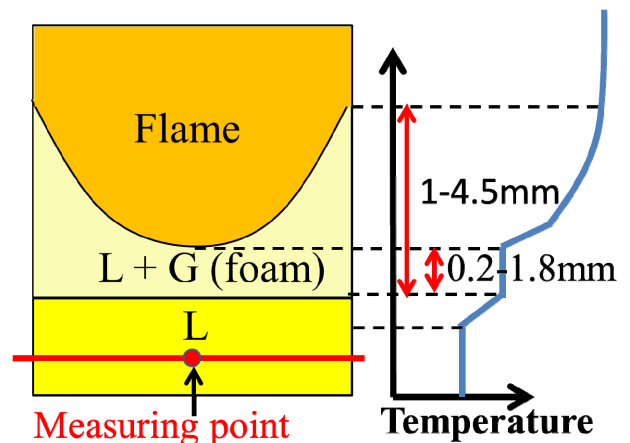


Fig. 12. Comparison of foam shape with temperature distribution.

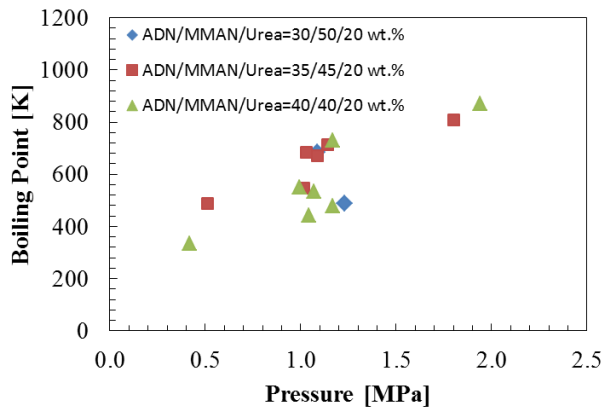


Fig. 13. Pressure dependence of boiling point of ADN-based ionic liquid propellant at each composition.

Figure 13 shows the dependence of boiling point on pressure at each composition. It is clear that the boiling point increases with increasing pressure in the same way as for usual monomolecular boiling points. The boiling point dependence is roughly the same between compositions. These are intrinsic curves of chemical substances in the gas-liquid phase and are equal to the vapor pressure curves. Thus, comparing vapor pressure curves of the ADN-based ILP and its components might be useful for identifying the chemical substances in the gas-liquid phase. Hence, the predictions of the boiling mechanisms in (a) and (b) might be verified. In order to compare the vapor pressure curves of the ADN-based ILP with those of gases considered in the predictions in detail, the vapor pressures of gases that contain the many species considered in the predictions must be calculated by numerical analysis or measured experimentally, which might be difficult in view of the gas' combustible nature. Currently, there are no such data to specify whether the boiling mechanism is (a) or (b).

However, thermal decomposition and evaporation of ADN and MMAN might take place at the same time, as in prediction (b), because the thermal decomposition temperatures of ADN (around 400 K)¹³⁾ and MMAN (around 523 K)¹⁴⁾ are close to their boiling points. To clarify the boiling mechanism in combustion, one effective method would be to collect the gas in the gas-liquid phase and analyze it by gas-chromatography or mass spectroscopy.

4.2. Combustion characteristics with respect to the gas phase

As discussed in section 4.1, combustion wave structure consists of liquid, gas-liquid, and gas phases. As the unburned gas should be pre-mixed gas, the simple formula of pre-mixture combustion in Eq. (2) can be applied to combustion in the gas phase. Mass conservation at steady-state is written as in Eq. (3).

$$v_G \sim 1 / \rho_G \sqrt{\lambda \omega / c_p} \quad (2)$$

$$\rho_L r = \rho_G v_G \quad (3)$$

Using Eqs. (1)–(3), Eq. (4) is obtained.

$$\omega \sim c_p \rho_L^2 r^2 / \lambda \propto a^2 P^{2n} \quad (4)$$

The proportionality constant a and pressure exponent n increase with increasing ADN content as confirmed in Fig. 2.

Hence, according to Eq. (4), the chemical reaction rate ω increases with increasing ADN content.

Figure 6 shows that the burned gas almost reaches the chemical equilibrium condition. According to the NASA CEA software, the main components at chemical equilibrium for the ADN-based ILP are H₂O, N₂, H₂, CO, and CO₂, in descending order of mole fractions. Thus, the burned gas would have nearly same composition.

4.3. Ignition characteristics

First, behavior before ignition in Figs. 8–10 are discussed. The formations of colored layers were observed near the lower ignition limit. One of the reasons for this observation is that the chemical reaction rate is slow at low pressure. Meanwhile, the reason for the formation of layers might be differences of specific weights between reaction products or stepwise reactions along the flow of products. The brownish or pale brownish layers were formed as shown in the right images of Figs. 8–10. These layers must contain NO₂ because the heat supplied to the propellant is insufficient for complete combustion, so incomplete combustion gases are generated. In particular, the ADN-based ILP at 40/40/20 wt. % has more oxidizer (in the form of ADN) than the other compositions. Therefore, the layer tends to be pale brownish in color as in the right image of Fig. 10 because generation of NO₂ decreases compared to the case for other compositions.

Finally, the dependence of the lower ignition limit on ADN content is discussed. Table 1 shows that the lower ignition limit decreases with increasing ADN content. Therefore, the composition with greater content of ADN is better in cases where vacuum ignition is required in the thruster chamber.

5. Conclusion

In order to understand the combustion mechanism of ADN-based ILP, which is of low volatility, the combustion wave structure was focused on in this study. The dependence of combustion and ignition characteristics on ADN content was also discussed. Hence, the temperature profiles in the combustion wave and linear burning rates were measured in strand burner tests at compositions of 30/50/20, 35/45/20, 40/40/20 wt. %.

First, the combustion wave structure was discussed. The combustion wave structure consists of liquid, gas-liquid, and gas phases. In the gas-liquid phase, there are two considerations: (a) volatile liquid, which is a pyrolyzed ADN-based ILP, might be evaporated; (b) ADN, MMAN, and urea might be evaporated and/or pyrolyzed into their neutral dissociation products through endothermic reactions. The dependence of boiling point on pressure characterizes chemical substances in the gas-liquid phase.

The second topic of focus is that of combustion characteristics with respect to the gas phase. According to the results of strand burner tests, the linear burning rate and pressure exponent increase with increasing ADN content between 30 – 40 wt. %. Therefore, the chemical reaction rate in the gas phase increases with increasing ADN content, given that pre-mixture combustion happens in the gas phase. The measured flame temperatures show that the burned gas is

almost in chemical equilibrium. Thus, its main constituents would be H₂O, N₂, H₂, CO, and CO₂.

The third point is ignition characteristics. Around the lower ignition limit, colored layers were observed on the ADN-based ILP owing to a low chemical reaction rate. After white gas was generated, a yellowish layer was observed. After that, the behaviors were different for each composition of the ADN-based ILP. Two layers were formed at 40/40/20 wt. %. Meanwhile, three layers were formed at the other two compositions. The reasons for the formation of layers could be differences of specific weights between chemical substances or stepwise reactions along the flow of products. The brownish or pale brownish layer was observed at all compositions. The brownish color indicates NO₂, which would be generated owing to incomplete combustion caused by insufficient heat supplied. Finally, the lower ignition limit decreases with increasing ADN content. A large fraction of ADN content might be one appropriate criterion for selection of composition.

References

- 1) Bombelli, V., Simon, D., Marée, T. and Moerel, J. L.: Economic Benefits of the Use of Non-Toxic Mono-propellants for Spacecraft Applications, AIAA Paper 2003-4783, 2003.
- 2) Larsson, A. and Wingborg, N.: Green Propellants Based on Ammonium Dinitramide (ADN), *Advances in Spacecraft Technologies*, J. Hall (Ed.), ISBN: 978-953-307-551-8, InTech, Rijeka, 2011, pp. 139–157.
- 3) Katsumi, T., Kodama, H., Matsuo, T., Ogawa, H., Tsuboi, N. and Hori, K.: Combustion Characteristics of a Hydroxylammonium Nitrate Based Liquid Propellant. Combustion Mechanism and Application to Thrusters, *Combust. Explo. Shock+*, **45**(4) (2009), pp. 442–453.
- 4) Ide, Y., Takahashi, T., Iwai, K., Nozoe, K., Habu, H. and Tokudome, S.: Potential of ADN-based Ionic Liquid Propellant for Spacecraft Propulsion, *Procedia Eng.*, **99** (2015), pp. 332–337.
- 5) Wilkes, J. S.: A Short History of Ionic Liquids—from Molten Salts to Neoteric Solvents, *Green Chem.*, **4** (2002), pp. 73–80.
- 6) Smiglak, M., Reichert, W. M., Holbrey, J. D., Wilkes, J. S., Sun, L., Thrasher, J. S., Kirichenko, K., Singh, S., Katritzky, A. R. and Rogers, R. D.: Combustible Ionic Liquids by Design: is Laboratory Safety Another Ionic Liquid Myth?, *Chem. Commun.*, **24** (2006), pp. 2554–2556
- 7) Heym, F., Etzold, B. J. M., Kern, C. and Jess, A.: An Improved Method to Measure the Rate of Vaporisation and Thermal Decomposition of High Boiling Organic and Ionic Liquids by Thermogravimetric Analysis, *Phys. Chem. Chem. Phys.*, **12** (2010), pp. 12089–12100.
- 8) Liaw, H. J., Chen, C. C., Chen, Y. C., Chen, J. R., Huang, S. K. and Liu, S. N.: Relationship between Flash Point of Ionic Liquids and their Thermal Decomposition, *Green Chem.*, **14** (2012), pp. 2001–2008.
- 9) Adams, G. K. and Stocks, G. W.: The Combustion of Hydrazine, Fourth Symposium (International) on Combustion, **4** (1953), pp. 239–248.
- 10) Vosen, S. R.: Hydroxylammonium Nitrate-Based Liquid Propellant Combustion-Interpretation of Strand Burner Data and the Laminar Burning Velocity, *Combust. Flame*, **82** (1990), pp. 376–388.
- 11) Katsumi, T., Hori, K., Matsuda, R. and Inoue, T.: Combustion Wave Structure of Hydroxylammonium Nitrate Aqueous Solutions, AIAA Paper 2010-6900, 2010.
- 12) Thakre, P., Duan, Y. and Yang, V.: Modeling of Ammonium Dinitramide (ADN) Monopropellant Combustion with Coupled Condensed and Gas Phase Kinetics, *Combust. Flame*, **161** (2014), pp. 347–362.
- 13) Lobbecke, S., Krause, H. H. and Pfeil, A.: Thermal Analysis of Ammonium Dinitramide Decomposition, *Propell. Explos. Pyrot.*, **22** (1997), pp. 184–188.
- 14) Miron, Y.: Thermal Decomposition of Monomethylamine Nitrate, *J. Hazard. Mater.*, **3** (1980), pp. 301–321.